Modelling and Simulation of Methanol Synthesis Reactor for Algerian Methanol Complex Case Study

Zineddine Boutekrabt[1], Rachida Chemini[1,*], Mansour Djabeur [2], Farid Aiouache[3]

[1]*Department of Chemical Engineering and Cryogenic, Faculty of Process and Mechanical Engineering, Laboratory of Theoretical and Applied Fluid Mechanics (LMFTA), University of Sciences and Technology Houari Boumediene (USTHB), Algiers, Algeria.* zboutekrabt@usthb.dz

[2]*Petrochemicals Division, Refining and Petrochemicals Activity, Algerian Methanol Complex CP1/Z, Oran, Algeria.* *Mansour.djabeur@sonatrach.dz*

[3]*Department of Engineering, Lancaster University, United Kingdom.* *f.aiouache@lancaster.ac.uk*

Email corresponding author: *rchemini@usthb.dz*

ABSTRACT

The growing economic importance of methanol has led to increased scientific interest in improving derivative products, such as formaldehyde and olefines, which represent the largest markets for methanol. At the industrial scale, methanol is produced from a syngas mixture of carbon monoxide, carbon dioxide, and hydrogen at low-pressure, using copper-based catalysts and operated under adiabatic or isothermal conditions. In this context, the present study investigates, through simulation, the effectiveness of two types of reactors: an adiabatic quench reactor currently operating at methanol plant in Arzew, Algeria, and a proposed multi-tubular isothermal reactor as an alternative. The performance of both reactors is assessed by observations of the concentration and temperature profiles. The results reveal an increase in methanol production in the multi-tubular reactor compared to the adiabatic quench reactor. A comparison of methanol production was analyzed, under the same operating conditions. The CO_2 conversion in the pseudo-isothermal reactor is 37.59% higher than the conversion rate obtained in the adiabatic reactor 7.79%. Methanol production is more efficient in isothermal technology, with 213 tons per day, compared to and 41 tons per day in the adiabatic reactor.

KEYWORDS: *Adiabatic, Aspen Hysys, Isothermal, Methanol, Reactor, Simulation.*

INTRODUCTION

Methanol is one of the most important products in the petrochemical industry. More than 90 plants are installed in the world with a total capacity of 186.07 million tons in 2024 and an annual growth rate of 6.8% [1]. Global production has increased steadily since 2000, rising from 31.63 million tons to 112.08 million tons in 2024, corresponding to an average annual growth rate of around 5.9% per year. During the same period, global demand reached 113.74 million tons in 2024, with an annual growth rate of 5.7% [2].

Methanol is well known for its numerous applications, including plastic manufacturing and chemical production such as formaldehyde [3], acetic acid [4], dimethyl ether, methyl tertiary–butyl ether, and methylamine [5]. It is considered a critical intermediate in the synthesis of a variety of products encountered in daily life, including

resins, silicones, adhesives, antifreeze, and paints [6]. Methanol is also used as a fuel additive [7] and as a solvent [8]. Moreover, it is considered one of the most promising renewable alternatives to gasoline [9], due to its low carbon footprint [10,11].

Many technologies have been developed over the years to produce methanol from various sources, namely natural gas [12], coal [13,14], biomass [15], and carbon dioxide [16]. At the industrial scale, methanol is typically produced from the catalytic conversion of syngas (a mixture of CO, CO_2 and H_2 obtained by steam-reforming of natural gas). Nowadays, methanol is produced using low-pressure technology (i.e. 5-10 MPa) and at a temperature of 230-250°C [17]. The most common industrial catalyst is a $CuO/ZnO/Al_2O_3$ formulation, whose composition depends on the manufacturer [18]. Technologies developed by Imperial Chemical Industries (ICI) [19] and Lurgi [20] dominate the global market, operating low-pressure adiabatic or isothermal reactors [21].

The models used for the synthesis of methanol catalysed by commercial $CuO/ZnO/Al_2O_3$ catalysts [22,23] are classified into pseudo-homogeneous models, which assume a single phase in a plug-flow reactor (PFR) [24], and heterogeneous models, which consider distinct fluid and solid catalytic phases in a packed-bed reactor (PBR), both associated with models of flow dispersion. The pressure drops in a packed bed of catalyst are considered using the classical models of flow in the porous media, and the transport phenomena of mass and heat by convection in the fluid and diffusion inside the solid phases are estimated using lumped models of transfer coefficients and effectiveness factor [25,26].

Many researchers have focused on the modeling and optimization of methanol synthesis in packed-bed reactors [27]. Hoseiny et al. [28] investigated the effect of operating parameters on methanol synthesis using process modeling, including the influence of inlet temperature and the mole fractions of CO and CO_2 on methanol production. The operating conditions of a plant were optimized using response surface methodology (RSM) in a MATLAB environment, and the statistical analysis results indicated a potential 7% increase in production rate under the optimal operating conditions.

Lovik [29] studied the modeling and optimization of methanol synthesis, taking into account catalyst deactivation. A heterogeneous mass balance model was considered more rigorous than a pseudo-homogeneous reactor model. This approach, coupled with a recycle stream was adopted, and a sensitivity analysis was performed on key model parameters, such as the recycle rate and coolant temperature. The study concluded that the pseudo-steady state was more accurate after validation with an industrial process.

Nacer et al. [30] investigated a multi-fixed-bed quench reactor under steady-state operation using a heterogeneous mathematical model that accounts for the coupling of chemical reactions with complex kinetics and diffusion resistance. The model was solved using the Runge-Kutta method for the integration of bulk phase equations and the orthogonal collocation method for the diffusion equations. They reported that the conversion rate depends on the partial pressure of the CO_2/CO ratio, and proposed CO_2 injection into the feed to enhance methanol yield. Walid et al. [31] reported an improvement of methanol synthesis performance by substituting the quench reactor with a new Lurgi tubular reactor operated at industrially relevant conditions and confirmed the positive effect of CO_2 on methanol production.

The present paper reports an investigation, using process simulation of the performance of an adiabatic quench reactor for methanol synthesis operated at steady-state conditions, taking methanol produced at complex plant

CP1/Z in Arzew (Algeria) as a case study. The process design, reactor technology of the reactor, and model formulation along with a description of the operating parameters at the plant scale are presented.

The model is validated through a design case, and the performance of both the existing adiabatic technology and a proposed pseudo-isothermal alternative is further analyzed under the plant's current operating conditions. Performances were investigated in terms of conversion, reaction rate, temperature, concentration profiles, and overall process engineering.

THEORETICAL SECTION

Case study

The case study applies to the complex plant CP1/Z in Arzew, Algeria, which uses natural gas as the basic source for methanol production at low-pressure conditions. The process involves several stages, including steam-reforming of natural gas, methanol synthesis from syngas, and methanol purification by distillation (Fig.1). The reforming process of natural gas produces syngas by steam injection at a pressure of (3 MPa). The process is operated at a temperature of 850°C, pressure of (2 MPa), and in the presence of a nickel-based catalyst (NiO). The syngas is then subject to sequential operations of cooling and compression to 70°C and 53.7×10^5Pa, respectively, required by the methanol synthesis process.

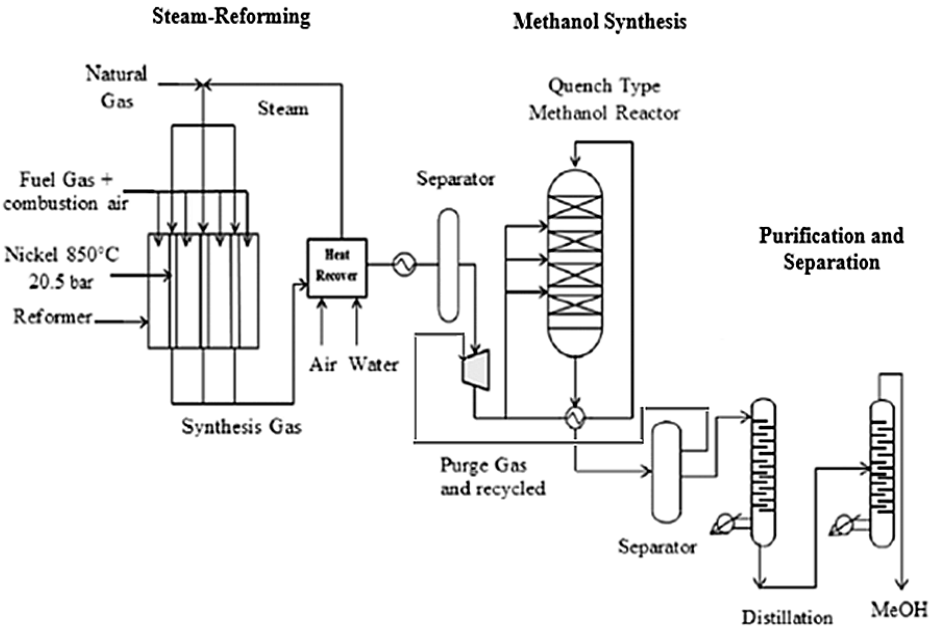

Fig. 1: Methanol synthesis process at complex plant CP1/Z.

Part of the obtained gas (between 60-75%) is pre-heated in a heat exchanger from 70°C to temperature 245°C before entering the adiabatic quench reactor, which contain four catalyst beds, while the other part (between 25-40% depending on the process case) of the syngas is used for cooling, in turn, is sub-divided into streams located between the beds, aiming to quench the reaction mixture at outlet of each catalytic bed. The crude methanol is then purified in two distillation columns in series, while water and the by-products (i.e. ethanol, dimethyl ether, and acetone) are removed to produce methanol grade A with a purity of 99.96% [32].

The reactor is operated adiabatically and contains multi-fixed beds with cooling achieved by gas quench injection (Fig.2), which lowers the temperature of the reactive mixture at the outlet of each bed and prevents the generation of undesirable hot spots in the catalyst bed, which in turn can result in catalyst deactivation through sintering of the active sites [33]. The reaction is favored at low pressure in the presence of a commercial copper-based catalyst of $CuO/ZnO/Al_2O_3$ formulation, which is highly sensitive to temperature variation.

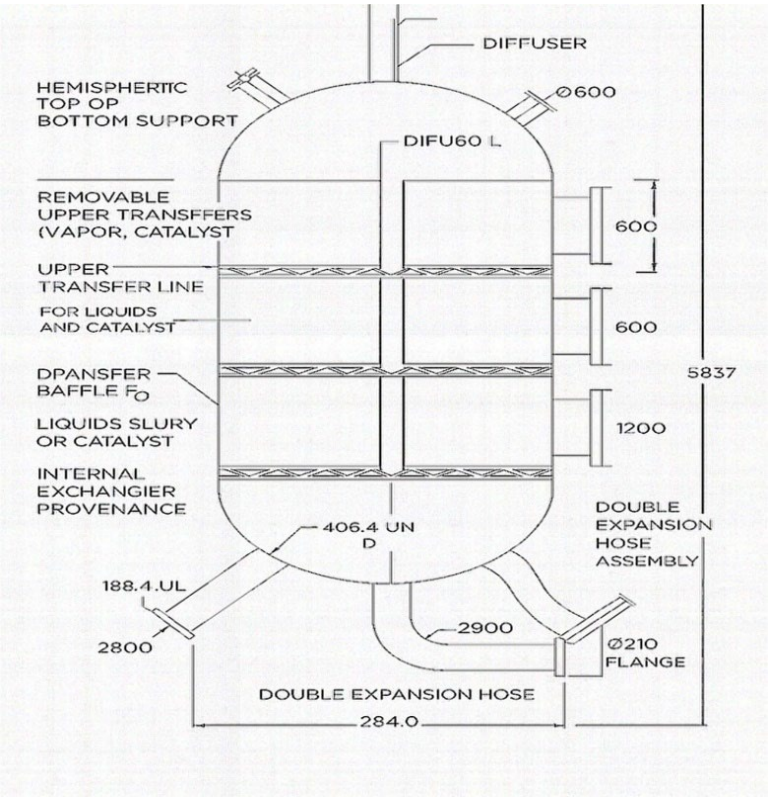

Fig. 2: Methanol synthesis reactor at complex plant CP1/Z.

The specifications of the commercial catalyst are summarized in Table 1 [32].

Table 1: Specifications of reactor and catalyst (manufacturer's data).

Parameters	Characteristics
Type of reactor	Adiabatic quench reactor
Number of beds	4
Reactor diameter *D* (m)	3.9
Reactor length *l* (m)	7.0
Height of catalytic bed (m)	0.75
Void fraction	0.38
Average pressure drops ΔP (10^5 Pa)	0.52
Type of catalyst	$CuO/ZnO/Al_2O_3$
Form	Tablets, granular
Catalyst dimensions (mm)	5.3 × 5.1

Composition (%)	CuO : 61 % ZnO : 28 % Al_2O_3 : 10%
Catalyst void fraction ε	0.24
Catalyst particle density ρ_b (kg/m³)	1700
Catalyst Lifetime minimum (years)	5

Tables 2 and 3 report the feed composition and operating conditions, respectively, along with the catalyst specifications, for design and real case operations at CP1/Z complex, Algeria [32].

Table 2: Molar composition (%) of syngas at the reactor inlet for design and real case operations at CP1/Z.

Components	Design case of CP1/Z plant (%)	Real case of CP1/Z plant (%)
CO	7.5	3.74
CO_2	6.0	4.61
H_2	73.7	77.81
CH_4	9.0	10.09
N_2	3.2	3.75
CH_3OH	0.5	00
H_2O	0.1	00

Table 3: Operating conditions at the reactor inlet for design and real case.

Parameters	Design case	Real case
Pressure (10^5 Pa)	53.7	43
Temperature (°C)	245	225
Total flow rate Q_T (Nm^3/h)	318 700	295 654
Flow rate of quench Q_Q (Nm^3/h)	95 910	60 812
Temperature of quench gas T_Q (°C)	70	42.5

Reactor Modeling and Validation

Many kinetic equations have been proposed for the reaction of methanol synthesis catalyzed by $Cu/Zn/Al_2O_3$ catalysts [21]. The overall mechanism of hydrogenation of syngas to methanol involves three main reactions: hydrogenation of CO (1), hydrogenation of CO_2 (2), and reverse water gas shift reactions (RWGS) (3) [33,34].

$$CO + 2H_2 \leftrightharpoons CH_3OH \qquad (\Delta H°298\text{K} = -90.77\ \text{kJ/mol}) \qquad (1)$$

$$CO_2 + 3H_2 \leftrightharpoons CH_3OH + H_2O \qquad (\Delta H°298\text{K} = -49.58\ \text{kJ/mol}) \qquad (2)$$

$$CO_2 + H_2 \leftrightharpoons CO + H_2O \qquad (\Delta H°298\text{K} = +41.19\ \text{kJ/mol}) \qquad (3)$$

The reactions (1) and (2) are exothermic and controlled by chemical equilibrium [35], requiring significant cooling to remove excess heat and shift the chemical equilibrium toward methanol production, while reaction (3) corresponds to the water gas shift reaction and is only mildly endothermic [36].

Graaf et al. [37,38] and Graaf and Beenackers [39] considered that methanol was produced from CO and CO_2 by successive hydrogenation over the hydrolysis reaction. Skrzypek et al.[40] suggested a reaction mechanism based on the water-gas shift reaction and the hydrogenation of CO_2. The Langmuir-Hinshelwood kinetic model was found suitable for low-pressure methanol synthesis, with higher CO_2 conversion observed compared to CO. Vanden and Froment [41] proposed a more detailed kinetics mechanism for syngas conversion catalyzed by $Cu/Zn/Al_2O_3$, confirming that CO_2 is the key reactant in methanol synthesis. Lim et al. [42] developed a kinetic model containing 48 reaction rates and reported the significant positive effect of CO_2 on methanol yield.

The kinetic model of Bussche and Froment [41] has been widely used in literature by many researchers such as Van-Dal and Bouallou [43], Pérez-Fortes et al. [44], Panahi et al. [45], Luyben [46], Chen et al. [47], and Walid et al.[31]. This model assumes that methanol is produced slowly by CO_2 hydrogenation, while water is formed by the reverse water gas-shift and has an inhibitory effect on the overall reaction.

On an industrial scale, CO_2 hydrogenation to produce methanol and the hydrolysis reactions are feasible within well-defined temperature ranges, pressures, and reactant compositions (Table 4).

Table 4: Operating conditions of methanol synthesis used by the model of Bussche and Froment.

Catalyst	Reaction	Flow molar fraction (%)	Temperature (K)	Pressure (10^5 Pa)	Type of reactor
$CuO/ZnO/Al_2O_3$	(1) $CO_2 + 3H_2 \leftrightharpoons CH_3OH + H_2O$ (2) $CO_2 + H_2 \leftrightharpoons CO + H_2O$	CO: 0-30 CO_2: 0-30 H_2: 70 $\rho CO_2/\rho CO$: 0-4.1	453-553	15-51	Tubular

The kinetic reactions are presented in Eqs. (4) and (5), and kinetic parameter models are listed in Table 5 [41].

$$r_{CH3OH} = \frac{F_3 P_{CO2} P_{H2}\left[1-\frac{1}{K_1^{eq}\left(\frac{P_{H2}P_{CH3OH}}{P_{CO2}P_{H2}^3}\right)}\right]}{\left[1+F_2\left(\frac{P_{H2O}}{P_{H2}}\right)+F_1\sqrt{P_{H2}}+K_{H2O}P_{H2O}\right]^3} \quad (4)$$

$$r_{RWGS} = \frac{K_1' P_{CO2}\left[1-K_2^{eq}\left(\frac{P_{H2O}P_{CO}}{P_{CO2}P_{H2}}\right)\right]}{\left[1+F_2\left(\frac{P_{H2O}}{P_{H2}}\right)+F_1\sqrt{P_{H2}}+K_{H2O}P_{H2O}\right]} \quad (5)$$

Table 5: Parameters of the kinetic model from Bussche and Froment 1996 [41]**.**

Parameters	Constants	A	B
F= A exp (B/RT)			
F1 (1/bar $^{1/2}$)		0.499	17 197
F2		3 453.38	0
F3 (mol/kg s bar²)		1.07	36 696
K= A exp (B/RT)			
K_1' (mol/kg s bar)		1.22×10^{-10}	-94 765
K_{H_2O} (1/bar)		6.62×10^{-11}	124 119

$K^{eq} = 10^{(A/T-B)}$			
K_1^{eq} (1/bar^2)		3066	10.592
K_2^{eq} (-)		2073	2.029

The kinetic model proposed by Bussche and Froment, which is adopted in the present work [28,31,49], was developed based on a commercial $CuO/Zn/Al_2O_3$ catalyst [49] and operated under feed conditions similar to those encountered in the CP1/Z plant.

At typical industrial conditions, the two reactions, namely the hydrogenation of CO_2 to obtain methanol and hydrolysis, take place exclusively on the copper phase of the catalyst. The kinetic model used for methanol synthesis reactor simulation is the Froment and Vanden Bussche model because it is the most favorable model for our case at CP1/Z complex.

Reactor Model

In the present work, the design was undertaken using a pseudo-homogeneous model based on material and energy balances. In this model, the following assumptions were considered for plug-flow reactor design:

- Negligible axial diffusion: the species dispersion in the reactor was not considered.
- Homogeneous catalyst particle: no temperature gradient or concentration within the particle.
- Parallel reactions are negligible due to the high selectivity of the catalyst.

Before the resolution of material and energy balances, the physicochemical properties of syngas are needed. These properties have been calculated by the methods cited elsewhere in Table 6.

Table 6: Methods used for calculating the physicochemical properties.

Property	***Method***
Gas mixture density	Poling et al., 2001 [50]
Gas viscosity	Perry and Green [51]
Mixed-gas viscosity	Wilke [52]
Gas conductivity	Perry and Green [51]
Mixed-gas conductivity	Mason and Saxena [53]
Mixed-gas heat capacity	Poling et al., 2001 [50]
Overall heat transfer coefficient	Froment and Bischoff [52]

Material balance:

The material balance applied to a differential mass of the packed bed reactor was applied to all components of the reaction mixture and is expressed by equations 6 to 12.

$$\frac{dF_i}{dW} = (r_i') \tag{6}$$

$$\frac{dF_{CO}}{dW} = r'_{2,MEOH} \tag{7}$$

$$\frac{dF_{CO_2}}{dW} = (-r'_{1,MEOH} - r'_{2,RWGS}) \quad (8)$$

$$\frac{dF_{H_2}}{dW} = (-3r'_{1,MEOH} - r'_{2,RWGS}) \quad (9)$$

$$\frac{dF_{H_2O}}{dW} = (r'_{1,MEOH} + r'_{2,RWGS}) \quad (10)$$

$$\frac{dF_{MEOH}}{dW} = r'_{1,MEOH} \quad (11)$$

$$P_i = \frac{F_i}{\sum F_i} * P \quad (12)$$

With i= CO, CO_2, H_2, H_2O, CH_3OH

Energy balance:

The heat transfer along the reactor can be evaluated based on the heat balance theory. For the design of the reactor, it is necessary to establish a temperature profile. The heat balance applied to the differential mass of the packed bed is expressed by Eq.13 [54].

$$\frac{dT}{dW} = \frac{\sum_{j=1}^{2}((-\Delta H_j) * (-r'_j)) - (\frac{U * a(T - Ts)}{\rho_c})}{\sum F_{i*} C_{Pi}} \quad (13)$$

Pressure drops:

The pressure drop can be calculated according to Ergun's equation with a correlation factor for a packed bed (Eq 14).

$$\frac{dP}{dZ} = -\frac{G}{\rho gc\, Dp} + \frac{(1-\varepsilon)}{\varepsilon^3}[\frac{150\,(1-\varepsilon)\mu}{Dp} + 1.75\, G \quad (14)$$

Thermodynamic model

On the other hand, the selection of the thermodynamic model was based on the design data of CP1/Z, the molar composition of the feed at the reactor inlet, and the operating parameters reported in Tables 2 and 3 [32].

The reactive mixture contains polar components that generate mutual interactions, which, once aggregated, lead to a deviation from the ideal behavior of thermodynamic properties reflected by the activity coefficients [55]. Two models of prediction of activity coefficients, namely the Universal Quasi Chemical (UNIQUAC) and Non-Random Two-Phase (NRTL) [56], were tested for the liquid phase, while the Peng-Robinson equation of state [57] was adopted to model the fugacity properties of the gaseous phase [50].

The simulation results are summarized in Table 7.

Table 7: Molar composition at the outlet of the reactor between design plant case, real case operation of CP1/Z, and simulation results of adiabatic quench reactor.

Components	Design case (%)			Real case (%)		
	Data	Simulation	Error	Data	Simulation	Error
CO	6.0	6.16	2.66	2.99	2.40	19.73
CO_2	5.3	5.24	1.14	4.10	3.48	15.12
H_2	71.1	71.08	0.02	68.30	75.08	9.92
CH_4	9.5	9.52	0.21	16.69	10.69	35.94
N_2	3.4	3.38	0.22	4.14	3.97	4.10
CH_3OH	3.5	3.41	2.50	3.20	2.97	7.18
H_2O	1.2	1.21	0.84	0.58	1.4	1.43

Where Ts is the temperature of the surroundings, the set of mass and energy balance equations was solved using the Newton method embedded in Aspen Hysys.

A preliminary quantitative analysis of the results of the adiabatic quench reactor, based on a plug flow model with negligible flow dispersion implemented in the commercial Aspen Hysys software, is presented in Table 7. This table contains both the design and real operation data of the CP1/Z plant and indicates that, unlike the real case model with an average deviation of 13.35%, the design case operation with an average deviation of 1.08% is well predicted by the model. Consequently, the model describing the best composition in the multiphase system, the UNIQUAC model and the Peng-Robinson equation of state were adopted for the remainder of the study [58].

The design data were used to verify and validate the reactor process simulation. A difference of approximately 1% was observed between the simulation results obtained using Aspen HYSYS and the design data of the CP1Z complex. A difference of about 13% was observed between the simulation results obtained under design conditions and those obtained under real operating conditions for the adiabatic quench reactor. This deviation, which remains below 15%, can be attributed to several factors, including equipment aging and degradation, particularly of the reactor, as well as changes in operating conditions.

Adiabatic Quench Reactor and Multi-tubular Reactor Simulation

The performance of a reactor under pseudo-isothermal operations was then investigated, and the results were compared with those obtained under the existing adiabatic quench reactor at methanol plant CP1/Z.

The adiabatic quench reactor was simulated using thermodynamic data (C_{pi}, ρ_i presented in Table 9) embedded in Aspen Hysys software, along with the reactor design characteristics listed in Table 10. The plug flow model was adopted with negligible axial dispersion due to the high flow rates and the reduced impact of the wall on potential channeling in the neighborhood zones. The gas quench was introduced at the end of each bed section. The flow diagrams of the adiabatic and pseudo-isothermal reactor simulations are shown in Figs 3a and 3b, respectively.

(a)

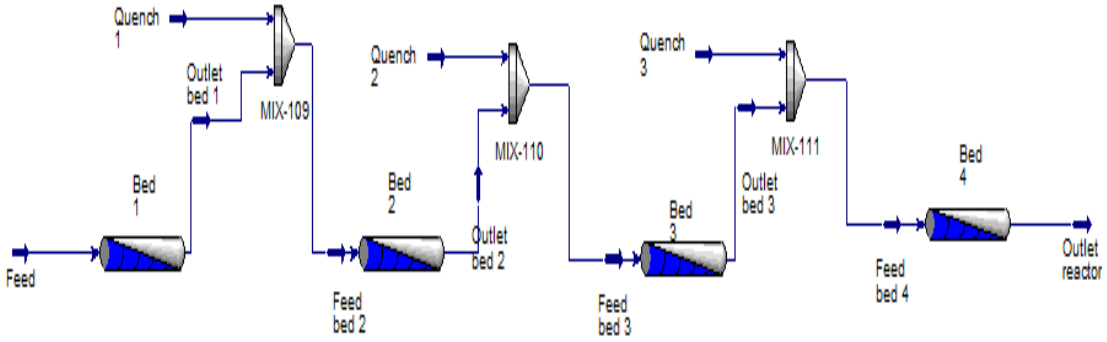

(b)

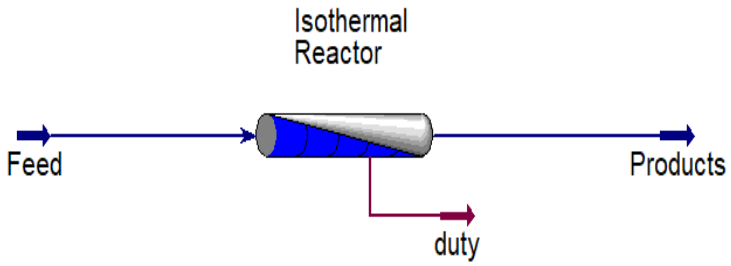

Fig. 3: Flow diagram: (a) Adiabatic quench reactor, (b) Isothermal reactor.

The pseudo-isothermal reactor consists of a shell and tube heat exchanger. The synthesis gas is circulated on the tube side, while the cooling water flows on the shell side at its boiling temperature. The design of an isothermal reactor based on a judicious strategy for temperature control and heat recovery would promote higher syngas conversion by mitigating the limitation imposed by chemical equilibrium.

RESULTS AND DISCUSSION

The model was first validated using operating conditions of the adiabatic quench reactor and was then extended to simulate the proposed multi-tubular reactor configuration operated under similar operating conditions. The corresponding performance was subsequently analyzed, as presented in the following sections.

Performance of Adiabatic Quench Reactor and multi-tubular Reactor

Concentration profile of CO_2, H_2, H_2O and CH_3OH

In the adiabatic quench reactor, a steady decrease in the molar fraction of CO_2 and H_2 is observed in the first bed, as shown in Figures 4a and 4b. CO_2 and H_2 are consumed through exothermic reactions to produce CH_3OH and H_2O. Consequently, a gradual increase in the molar fraction of methanol and water is observed, as illustrated in Figs 4c and 4d, favored by the temperature rise and the high concentration of reactants. The injection of the quench gas effectively maintained the operating temperatures positively, which maximized the conversion to 0.0033 mole fraction of methanol.

In the pseudo-isothermal reactor, the molar fraction of CO_2 and H_2 decreased along the reactor length by 0.0298 and 0.7522, respectively, while the fraction of CH_3OH and H_2O increased progressively. At the outlet, the methanol molar fraction reached 0.018.

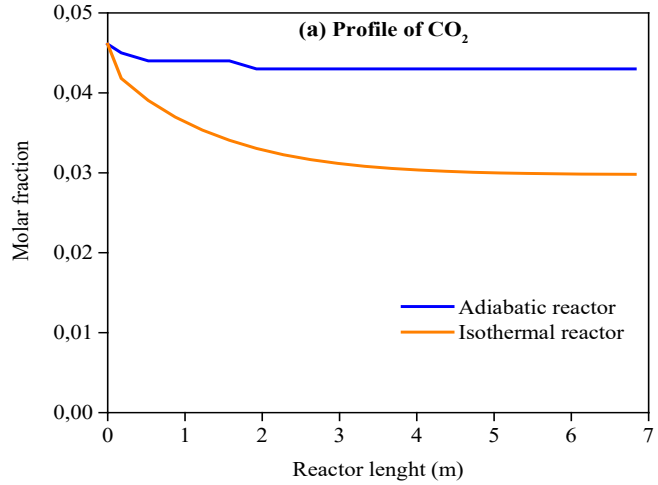

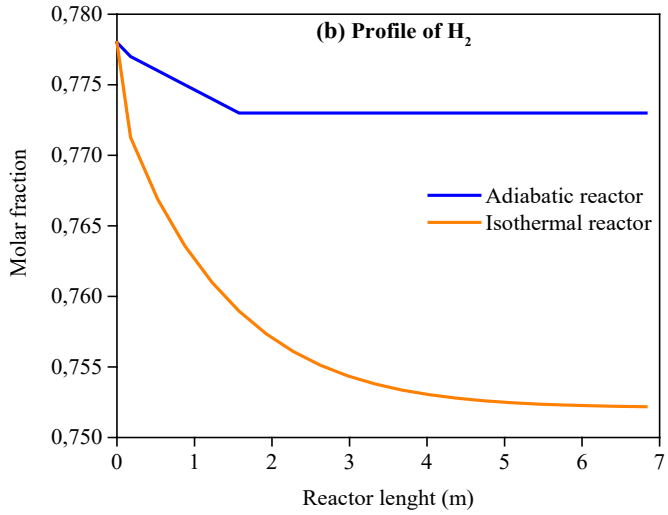

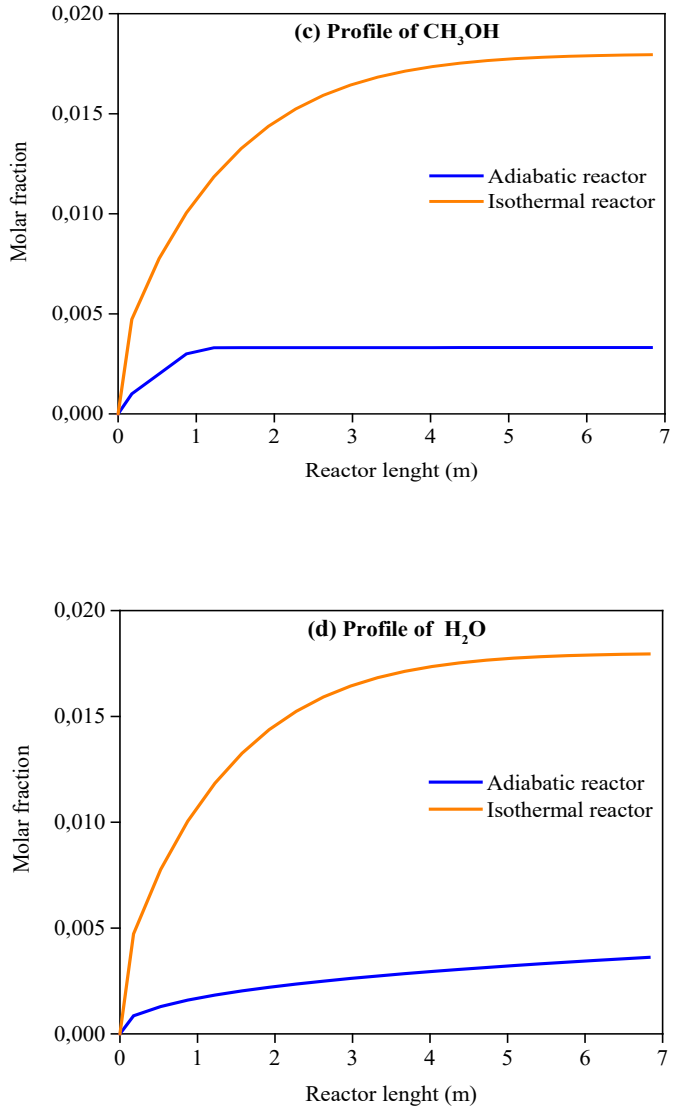

Fig. 4: Concentration profiles of components in adiabatic quench reactor and isothermal reactor

(a) Profile of CO_2, (b) Profile of H_2, (c) Profile of CH_3OH, (d) Profile of H_2O.

Overall, CO_2 and H_2 conversion was significantly higher in the isothermal reactor compared with the adiabatic quench reactor. The methanol mol fraction obtained in the isothermal and adiabatic quench reactor was 0.018 and 0.0033, respectively. At the reactor outlet, the mass flow rate of CH_3OH was 1692.88 Kg/h for the adiabatic quench reactor, and 8831.4 Kg/h for the pseudo-isothermal reactor.

Reaction Rate Profile

Fig.5 shows the variations of the reaction rate along the adiabatic quench reactor and the pseudo-isothermal reactor. At the early stage of the reactor length, the reaction takes place in the direction of CO_2 consumption; thus, the kinetic profile decreased, and methanol was mainly produced in the first bed, where the CO_2 conversion rate was high in comparison with the isothermal configuration, which exhibits a gradual decrease in reaction rate. In the

isothermal reactor, the CO_2 conversion rate was around 37.59%, taking place steadily along the length of the reactor.

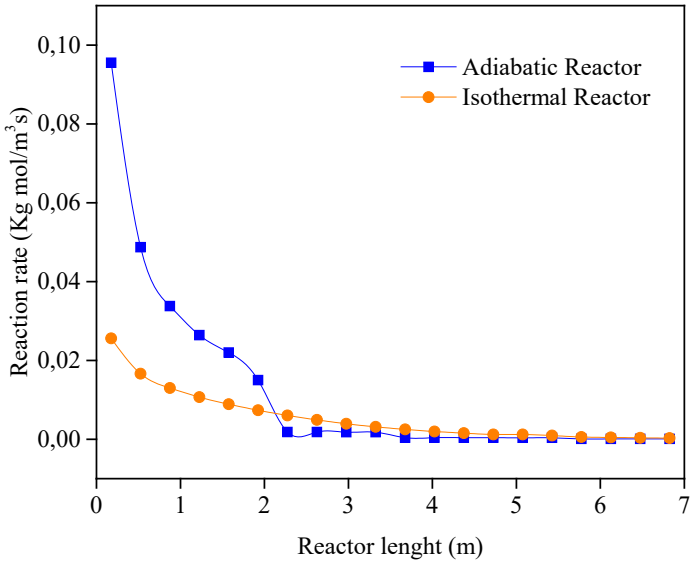

Fig. 5: Reaction rate profile of muti-tubular and adiabatic quench reactor.

Temperature profile

Fig.6 shows the temperature profile in the adiabatic quench reactor, exhibiting a steady increase along the reactor length. In the first catalytic bed, a significant temperature rise (ΔT= 8-9°C) is observed between the bed inlet and outlet (225-233°C), due to the exothermicity of the hydrogenation reaction. This temperature gradient decreases subsequently, following the reaction rate profile-illustrated in Fig. 4. The gas quench injected between the catalyst beds helps to reduce the bed temperature within the limits imposed by the reaction kinetics and the adiabatic thermodynamic equilibrium constrained by catalyst deactivation. At the outlet, the temperature reaches 200.3°C, corresponding to a total gradient of 24.7°C relative to the inlet.

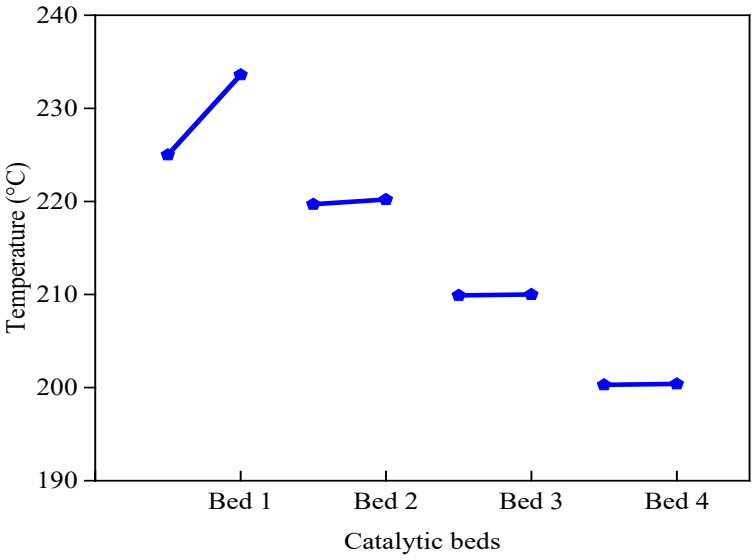

Fig.6: Temperature profile along adiabatic quench reactor.

Fig.7 shows the variation of the temperature profile in a pseudo-isothermal reactor. The temperature increases progressively, reaching a maximum of 257°C at a length of 3m. After this point, the temperature stabilizes along the reactor length. At the start of the reaction, under transient conditions, both the reaction fluid and the reactor are below the target reaction temperature. Catalyst, heat transfer fluid are not at equilibrium thermal, the temperature increases, then stabilizes along the reactor isothermal. There is no difference between the tube side and shell side temperature because the coefficient of thermal exchange is higher, and thermal resistance is negligible.

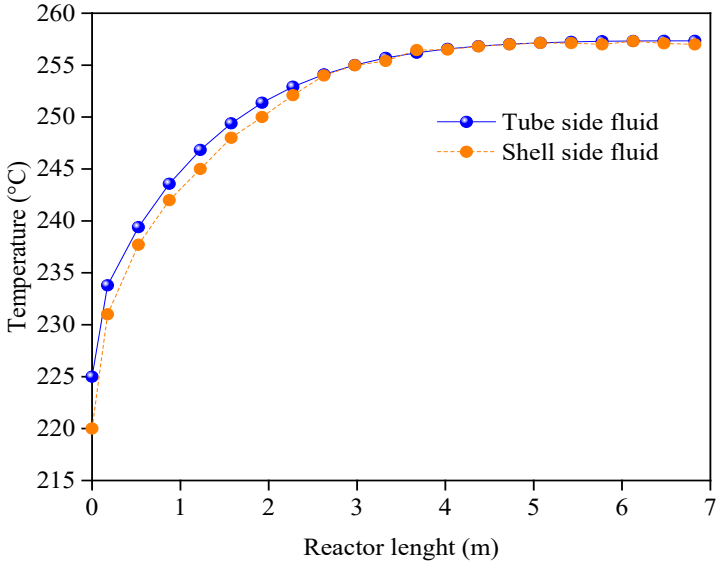

Fig.7: Temperature profile of multi-tubular reactor.

Comparison of performance of the multi-tubular and the adiabatic Reactor

Based on the simulation results for the adiabatic quench reactor and the pseudo-isothermal reactor, Table 8 compares the molar fractions at the outlet of each reactor.

Table 8: Molar fraction of components at the outlet of multi-tubular and adiabatic quench reactor.

Components	Molar fraction at the outlet of multi-tubular reactor (%)	Molar fraction at the outlet of Adiabatic quench reactor (%)
CO	3.87	3.76
CO_2	2.98	4.31
H_2	75.22	77.33
CH_4	10.45	10.16
N_2	3.88	3.77
CH_3OH	1.80	0.33
H_2O	1.80	0.33

In the case study, and under the same operating conditions, as shown in Table 8, the methanol molar fraction at the outlet of the pseudo-isothermal reactor (i.e. 0.018) is significantly higher than that of the adiabatic quench reactor (0.0033). The CO_2 conversion in the pseudo-isothermal reactor is 37.59%, roughly four (4) times higher than the conversion rate obtained in the adiabatic reactor 7.79%.

The performance of the two approaches in terms of conversion and methanol production is summarized in Table 9. The implantation of pseudo-isothermal technology at Algerian Methanol Complex CP1/Z would allow for the production of more than 172 tons per day compared to the existing adiabatic technology.

Table 9: Methanol production with adiabatic quench and pseudo-isothermal reactors.

Simulation Results	Adiabatic quench Reactor	Pseudo-isothermal Reactor
Methanol molar fraction at the outlet of reactor (%)	0.33	1.80
Conversion rate of CO_2 (%)	7.79	37.59
Methanol mass flow (Kg/h)	1681.8	8832.2
Methanol production (Tons/day)	41	213

These results highlight the significance of the thermodynamic limitation in the case of the adiabatic quench reactor, which could be remedied by a cost-effective flow recycling strategy. In contrast, the pseudo-isothermal reactor appears to operate more effectively as it is favored by the achievement of lower temperature via thermal cooling.

Sensitivity analysis of the model

Effect of Inlet Temperature

The effect of inlet temperature on methanol production was investigated for both the adiabatic quench and pseudo-isothermal reactors.

Fig. 8 shows a strong correlation between the reactor operating temperature and CO_2 conversion. Unlike the pseudo-isothermal reactor, where methanol production is relatively stable, the adiabatic reactor is strongly favored by inlet temperature. Operating at temperatures above 245°C is favorable for the adiabatic quench reactor. However, at a pressure of 43×10^5 Pa and a temperature of 253°C, methanol production is practically the same with the two technologies (i.e. 7.4 tons per hour).

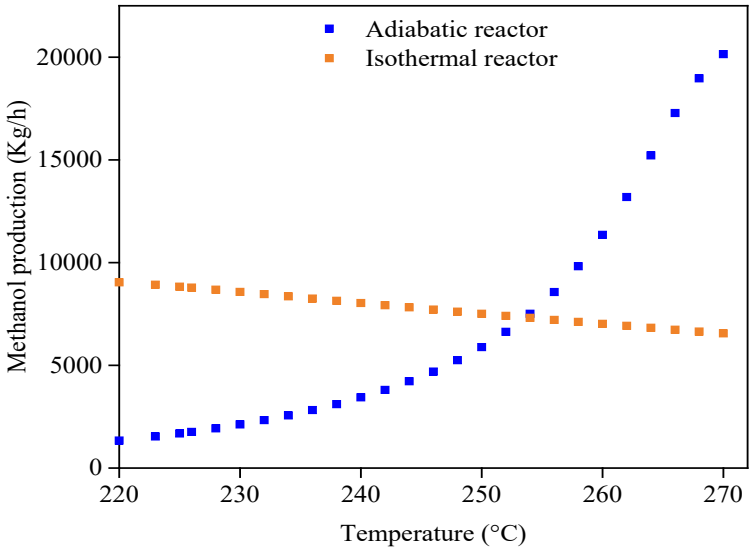

Fig. 8: Effect of inlet temperature on methanol production.

Operating at a temperature between 250°C and 260°C would be favorable for methanol production in the adiabatic quench reactor, while taking into account the 270°C limit recommended by the methanol complex CP1/Z and confirmed by the manufacturer of $CuO/ZnO/Al_2O_3$ catalyst (commercial catalyst of CP1Z plant). Interestingly, operating at low temperatures, between 220°C and 235°C, could achieve production as high as 9 tons per hour.

Effect of the Feed Composition on Methanol Production

Recent studies [28,29] have investigated methanol production from CO_2 to improve the performance of tubular reactor, and to confirm the theory of Vanden Bussche and Froment [41]. The effect of CO_2 in the feed syngas on methanol production was examined.

In this context, the positive influence of CO_2 on methanol yield is of particular interest. The approach consists of varying the molar composition of CO_2 and CO without affecting the composition of other components. The total fraction of CO_2 and CO content in the syngas at the reactor inlet is about 8.35%.

Fig. 9 shows that the CO_2/CO ratio as a key positive factor in methanol synthesis, confirming previous finding [31]. The actual CO_2/CO ratio was set to 1.23 and the production was about 1692.88 Kg/h. Setting a CO_2/CO ratio to values higher than 2 would valorize the CO_2 contained in the syngas via the water-gas-shist reaction.

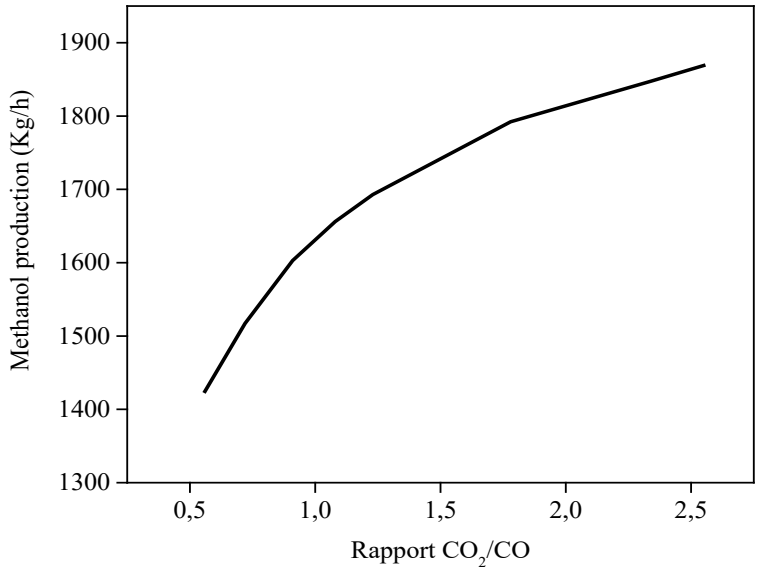

Fig. 9: Effect of CO_2/CO ratio in feed composition on methanol production in adiabatic quench reactor.

Effect of the Feed Pressure on Methanol Production

The variation of methanol production as a function of inlet pressure for both the adiabatic and pseudo-isothermal reactors is represented in Fig.10. The result confirms the positive impact of increased pressure on methanol production up to 60×10^5 Pa in the isothermal reactor, which compensates for the reduction in total flow rates by the change in the total stoichiometric number of the reactions.

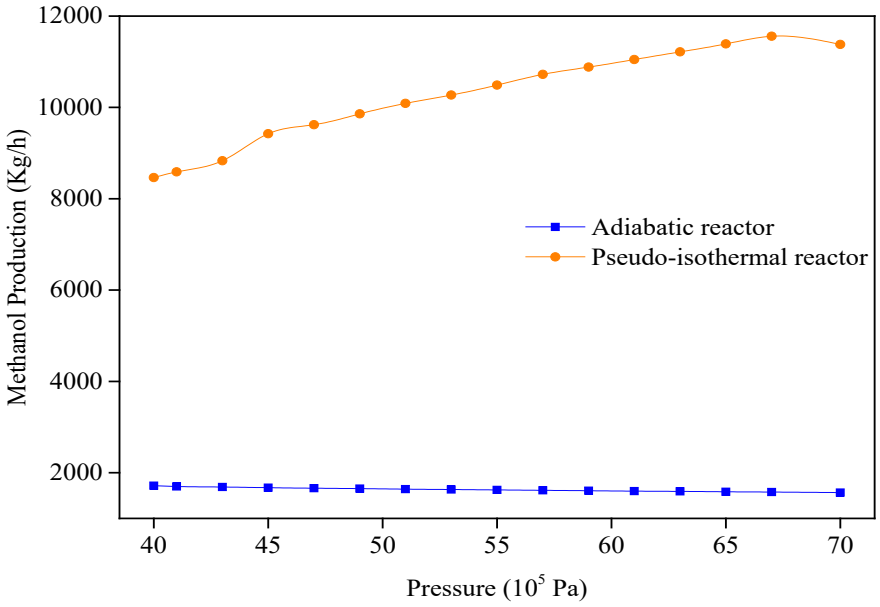

Fig. 10: Effect of inlet pressure on methanol production.

Increasing pressure enhances the production of methanol in Isothermal configurations for thermodynamic and kinetic reasons related to the synthesis reaction. In the adiabatic reactor, pressure has almost no effect on the production rate.

Based on the results obtained and the beneficial effect of inlet pressure on methanol production in an isothermal configuration, this reactor was optimized in terms of enhanced conversion rate and production of methanol in CP1/Z complex by proposing to increase pressure from 42.5 $\times 10^5$ Pa to 60 $\times 10^5$ Pa.

Methanol Production at Methanol Complex CP1/Z, Algeria

Tables 10 and 11 present the design parameters of the multi-tubular reactor following an optimization study by using Aspen Hysys module. The study takes into account the operating constraints at the Algerian methanol complex CP1/Z, the syngas composition, and the commercial catalyst used, with its characteristics given in the previous section.

Table 10: Operating parameters of the multi-tubular reactor.

Input parameters	Values
Flow rate Q (Nm^3/h)	318 700
Pressure P (10^5 Pa)	60
Temperature (°C)	230
Tube side temperature T_T(°C)	260
Shell side temperature T_s (°C)	250
Heat transfer coefficient on the shell side U (kJ/h m °C)	627
Heat capacity of water *Cp* (kJ/kmol °C)	82.45

Table 11: Characteristics of catalyst and multi-tubular reactor.

Parameters	Values
Internal diameter of the tube D_{Ti} (m)	0.03
External diameter of the tube D_{Te} (m)	0.035
Tube length l (m)	7
Void fraction (ε)	0.38
Catalyst particule density ρ_b (kg/m^3)	1700

The results presented in Table 12 indicate favorable conditions for methanol production at a temperature of 230°C and pressure of 60 10^5 Pa, resulting in a methanol production rate of 255 tons per day and a CO_2 conversion of 45.39%. The inlet temperature of the cooling fluid was maintained at 250°C, with a heat exchange surface area of 6864.6 m^2 corresponding to 8892 tubes in the multi-tubular reactor.

Table 12: Simulation results of multi-tubular reactor.

Parameters	Simulation Results
CO_2 conversion rate (%)	45.39
Tubes number	8892
Heat exchange coefficient (kJ/h m^2 °C)	1.827×10^4
Transfer coefficient Inside tubes (kJ/ h m °C)	1.163×10^6
Quantity of heat exchanged (kJ/h)	2.199×10^9
Pressure drops (10^5 Pa)	0.73
Methanol production (Tons per day)	255

CONCLUSION

The objective of this study was to enhance methanol production at Algerian Methanol Complex CP1/Z in Arzew, Algeria, by increasing the CO_2 conversion rate. A steady-state simulation study was carried out using Aspen Hysys to compare the performance of an adiabatic quench reactor and a pseudo-isothermal reactor proposed.

The simulation model was based primarily on design data rather than current plant real data measurement due to the effect of aging on catalyst effectiveness, packing beds, and overall reactor configuration and structure.

The results indicate that the pseudo-isothermal reactor is significantly more efficient, achieving CO_2 conversion of 37.59% compared to 7.79% for the adiabatic reactor. The Optimization of the process parameters for the pseudo-isothermal reactor could increase CO2 conversion to around 45.39%, and increase methanol production by around 200 tons/day relative to the current adiabatic reactor of methanol synthesis operated at Algerian methanol complex CP1/Z.

The substitution of the adiabatic reactor with an isothermal reactor appears to be a promising solution and strategy for improving methanol production at the CP1/Z complex. This solution not only addresses the challenges associated with aging reactors in the petrochemical industry but also contributes to the valorization of CO_2, supporting both operational efficiency and environmental sustainability.

Acknowledgement

The authors thank the Algerian Methanol Complex CP1Z of the company Sonatrach for their continuous support in data and process.

Nomenclature

A	Exchange surface area	(m^2)
C_p	Heat capacity of water	(kJ/kmol K)
D	Reactor diameter	(m)
l	Reactor length	(m)
D_{Ti}	Internal diameter of the tube	(m)
D_{Te}	External diameter of the tube	(m)
N	Tubes number	(-)
Q_T	Total flow rate	(Nm^3 /h)
Q_Q	Quench flow rate	(Nm^3/h)
F_3	Reaction rate constant	(mol/kg s bar^2)
F	Total molar flow rate	(mol/s)
U	Heat transfer coefficient on the shell side	(kJ/h m^2 K)
ΔH	Heat of reaction, reaction j	(kJ/mol)
ΔP	Pressure drop	(Pa)
K_1'	WGS Reaction rate constant	(mol/kg s bar)
K_i	Adsorption constant of species *i*	
K_1^{eq}	Equilibrium constant	($1/bar^2$)
K_2^{eq}	Equilibrium constant	(-)
l	Tube length	(m)
P	Pressure	(Pa)
T	Temperature	(°C)
T_Q	Quench temperature inlet reactor	(°C)
T_s	Tube side temperature	(°C)
T_{Ts}	Shell side temperature	(°C)

Abbreviation

CP1/Z	Petrochemical Complex in Arzew (Oran), Algeria
ICI	Imperial Chemical Industries
MTBE	Methyl tertiary-butyl ether
DME	Dimethyl Ether
RWGS	Reverse Water Gas-Shift reaction
UNIQUAC	Universal Quasi Chemical
NRTL	Non-Random Two Phase
PR	Peng-Robinson
PFR	Plug Flow Reactor

Greek letters

ε	Bed void fraction	(-)
ρ_b	Catalyst particule density	(kg/m^3)

REFERENCES

[1] Methanol-Methanol Market Services Asia (MMSA), accessed Oct. 01, 2025.

[2] Methanol Institute, methanol-price-supply-demand, accessed Jul. 27, 2025.

[3] Olaniyi A., Abidoye O., Awwal M., Modeling and Simulation of Partial Oxidation of Methanol to Formaldehyde on FeO / MoO 3 Catalyst in a Catalytic Fixed Bed Reactor, *Iran. J. Chem. Chem. Eng. (IJCCE)*, **40 (6):** 1800-1813 (2021).

[4] Behbahani M., Improvement of Homogeneous Catalysts for Methanol Carbonylation to Acetic Acid : Effects of Three-Ethyl Phosphine and Three-Phenyl Phosphine as Ligands, I*ran. J. Chem. Chem .Eng. (IJCCE)*, **44 (4):** 1033-1041 (2025).

[5] Dalena F.,Senatore A.,Marino A.,Gordano A.,Basile M., Basile A., Methanol Production and Applications: An Overview, *Methanol Elsevier*, 3–28 (2018).

[6] Bertau M.,Offermanns H.,Plass L.,Schmidt F.,Wernicke H.J., Methanol: The basic chemical and energy feedstock of the future: Asinger's vision today, Asinger's Vision Today, (2014).

[7] Olah G.A., Beyond oil and gas: The methanol economy, *Angew. Chemie - Int. Ed*, **44 (18):** 2636–2639 (2005).

[8] Ali K.A.,Abdullah A.Z., Mohamed A.R., Recent development in catalytic technologies for methanol synthesis from renewable sources: A critical review, *Renew. Sustain. Energy Rev*, **44:** 508–518 (2015).

[9] Olah G.A., Goeppert A., Prakash G. K. S., Beyond Oil and Gas: The Methanol Economy: Second Edition, Wiley-VCH, (2009).

[10] Metzger J.O., Beyond Oil and Gas: The Methanol Economy, *Angew. Chemie Int. Ed*, **45 (31):** 5045–5047 (2006).

[11] Ott. J., Gronemann V., Pontzen F., Fiedler E., Grossmann G., Kersebohm D.B., Weiss G., Witte C., Methanol, *Ullmann's Encycl. Ind. Chem*, (2012).

[12] Dalena F., Senatore A.,Basile M., Knani S., Basile A., Iulianelli A., Advances in Methanol Production and Utilization, with Particular Emphasis toward Hydrogen Generation via Membrane Reactor Technology, *Membr,* **8 (4):** 98 (2018).

[13] Balopi B., Agachi P., Danha, Methanol Synthesis Chemistry and Process Engineering Aspects- A Review with Consequence to Botswana Chemical Industries, *Procedia Manuf*, **35:** 367–376 (2019).

[14] Suganal, Huda M., Study on coal to methanol of Arutmin coal, *IOP Conf. Ser. Earth Environ. Sci*, **882 (1)** (2021).

[15] Pirola C., Bozzano G., Manenti F., Fossil or Renewable Sources for Methanol Production?, *Methanol Sci. Eng*, 53–93 (2020).

[16] Ganesh I., Conversion of carbon dioxide into methanol – a potential liquid fuel: Fundamental challenges and opportunities (a review), *Renew. Sustain. Energy Rev*, **31:** 221–257 (2014).

[17] Lange J.P., Methanol synthesis: a short review of technology improvements, *Catal. Today*, **64 (1–2):** 3–8 (2001).

[18] Klier K., Chatikavanij V., Herman R.G., Simmons G.W., Catalytic synthesis of methanol from COH2: IV. The effects of carbon dioxide, *J. Catal*, **74 (2):** 343–360 (1982).

[19] Sheldon D., Methanol production - A technical history, *Johnson Matthey Technol. Rev*, **61 (3):** 172–182 (2017).

[20] Méthanol basse pression (BP) | Air Liquide, accessed Oct. 01, 2022.

[21] Bozzano G., Manenti F., Efficient methanol synthesis: Perspectives, technologies and optimization strategies, *Prog. Energy Combust. Sci*, **56 :** 71–105 (2016).

[22] Riaz A., Zahedi G., Klemeš J.J., A review of cleaner production methods for the manufacture of methanol, *J. Clean. Prod*, **57:** 19–37 (2013).

[23] Abashar M.E.E., Al-Rabiah A.A., Investigation of the efficiency of sorption-enhanced methanol synthesis process in circulating fast fluidized bed reactors, *Fuel Process. Technol*, **179:** 387–398 (2018).

[24] Lommerts B.J., Graaf G.H., Beenackers A.A.C.M., Mathematical modeling of internal mass transport limitations in methanol synthesis, *Chem. Eng. Sci*, **55 (23):** 5589–5598 (2000).

[25] Shahrokhi M., Baghmisheh G.R., Modeling, simulation and control of a methanol synthesis fixed-bed reactor, *Chem. Eng. Sci*, **60 (15):** 4275–4286 (2005).

[26] Manenti F., Cieri S., Restelli M., Considerations on the steady-state modeling of methanol synthesis fixed-bed reactor, *Chem. Eng. Sci*, **66 (2):** 152–162 (2011).

[27] Mäyrä O., Leiviskä K., Modeling in Methanol Synthesis, *Methanol Sci. Eng*, 475–492 (2018).

[28] Hoseiny S., Zare Z., Mirvakili A., Setoodeh P., Rahimpour M.R., Simulation–based optimization of operating parameters for methanol synthesis process: Application of response surface methodology for statistical analysis, *J. Nat. Gas Sci. Eng*, **34:** 439–448 (2016).

[29] Løvik. I, Modelling, estimation and optimization of the methanol synthesis with catalyst deactivation, 2001.

[30] Nacer A., Bouroudi S., Simulation du réacteur de synthèse de méthanol d'Arzew, *Oil Gas Sci. Technol. - Rev. l'IFP*, **61 (6):** 799–809 (2006).

[31] Walid B.A.B.T., Hassiba B., Boumediene H., Weifeng S., Improved Design of the Lurgi Reactor for Methanol Synthesis Industry, *Chem. Eng. Technol*, **41 (10):** 2043–2052 (2018).

[32] HUMPHREYS & GLASGOW LIMITED, *Manuel d'exploitation pour l'unité Méthanol de 300/340 Tonnes/Tour*, LONDON, ENGLAND, 1971.

[33] Palma V., Meloni E., Ruocco C., Martino M., Ricca A., State of the Art of Conventional Reactors for Methanol Production, *Methanol Sci. Eng*, 29–51 (2018).

[34] Leonzio G., Mathematical modeling of a methanol reactor by using different kinetic models, *J. Ind. Eng. Chem*, vol. **85:** 130–140 (2020).

[35] Graaf G.H., Sijtsema P.J.J.M., Stamhuis E.J., Joosten G.E.H., Chemical equilibria in methanol synthesis, *Chem. Eng. Sci*, **41 (11):** 2883–2890 (1986).

[36] Schittkowski J., Ruland H., Laudenschlenger D., Girod K., Kahler K., Kaluza S., Muhler M., Schlog R., Methanol Synthesis from Steel Mill Exhaust Gases: Challenges for the Industrial Cu/ZnO/Al2O3 Catalyst, *Chemie Ing. Tech.*, **90 (10):** 1419–1429 (2018).

[37] Graaf G.H., Stamhuis E.J., Beenackers A.A.C.M., Kinetics of low-pressure methanol synthesis, *Chem. Eng. Sci*, **43 (12):** 3185–3195 (1988).

[38] Graaf G.H., Winkelman J.G.M., Stamhuis E.J., Beenackers A.A.C.M., KINETICS OF THE THREE PHASE METHANOL SYNTHESIS, *Tenth Int. Symp. Chem. React. Eng*, 2161–2168 (1988).

[39] Graaf G.H., Beenackers A.A.C.M., Comparison of two-phase and three-phase methanol synthesis processes, *Chem. Eng. Process. Process Intensif*, **35 (6):** 413–427 (1996).

[40] Skrzypek J., Lachowska M., Moroz H., Kinetics of methanol synthesis over commercial copper/zinc oxide/alumina catalysts, *Chem. Eng. Sci*, **46 (11):** 2809–2813 (1991).

[41] VANDENBUSSCHE K., G. Froment G., A steady-state kinetic model for methanol synthesis and the water gas shift reaction on a commercial Cu/ZnO/Al2O3 catalyst, *J. Catal*, **161 (1):** 1–10 (1996).

[42] Lim H.W., Park M.J., Kang S.H., H. Chae J., Bae J.W.,Jun K.W., Modeling of the Kinetics for Methanol Synthesis using Cu/ZnO/Al2O3/ZrO2 Catalyst: Influence of Carbon Dioxide during Hydrogenation, *Ind. Eng. Chem. Res*, **48 (23):** 10448–10455 (2009).

[43] Van-Dal É.S., Bouallou C., Design and simulation of a methanol production plant from CO2 hydrogenation, *J. Clean. Prod*, **57:** 38–45 (2013).

[44] Pérez-Fortes M., Schöneberger J.C., Boulamanti A., Tzimas E., Methanol synthesis using captured CO2 as raw material: Techno-economic and environmental assessment, *Appl. Energy*, **161:** 718–732 (2016).

[45] Panahi P.N., Mousavi S.M., Niaei A., Farzi A., Salari D., Simulation of methanol synthesis from synthesis gas in fixed bed catalytic reactor using mathematical modeling and neural networks, *Int. J. Sci. Eng. Res*, **3 (2):** (2012).

[46] Luyben W.L., Design and Control of a Methanol Reactor/Column Process, *Ind. Eng. Chem. Res*, **49 (13):** 6150–6163 (2010).

[47] Chen L., Jiang Q., Song Z., Posarac D., Optimization of Methanol Yield from a Lurgi Reactor, *Chem. Eng. Technol*, **34 (5):** 817–822 (2011).

[48] Leonzio G., Zondervan E., Foscolo P.U., Methanol production by CO2 hydrogenation: Analysis and simulation of reactor performance, *Int. J. Hydrogen Energy*, **44 (16):** 7915–7933 (2019).

[49] Rahimpour M.R., Bahri P., Fathi Kaljahi J., Jahanmiri A., Romagnoli A., A dynamic kinetic model for methanol synthesis on deactivated catalyst, *Comput. Chem. Eng*, **22 (1):** S675–S678 (1998).

[50] Reid R.C., Poling B.E., Prausnitz J.M., THE PROPERTIES OF GASES AND LIQUIDS, Fourth Edition, McGraw-Hill, 1987.

[51] Factors C., Perry's Chemical Engineers' Handbook, McGraw-Hill Education.

[52] Wilke C.R., A Viscosity Equation for Gas Mixtures, *J. Chem. Phys*, **18 (4):** 517-519 (1972).

[53] Mason E.A., Saxena S.C., Thermal Conductivity of Multicomponent Gas Mixtures. II, *J. Chem Phys*, **511:** 2–6 (1959)

[54] Froment G.F., Bischoff K.B., Wilde J.D., Chemical Reactor Analysis and Design, USA, 2011.

[55] B. E. Poling B.E., Prausnitz J.M., O'Connel J.P., Properties of Gases and Liquids, Fifth Edition, McGraw-Hill, 2001.

[56] Kiss A.A, Pragt J.J., Vos H.J., Bargeman G., Groot M.T., Novel efficient process for methanol synthesis by CO2 hydrogenation, *Chem. Eng. J*, **284:** 260–269 (2016).

[57] Peng D.Y.,Robinson D.B., A New Two-Constant Equation of State, *Ind. Eng. Chem. Fundam*, **15 (1):** 59–64 (1976).

[58] Samiee L., GhasemiKafrudi E., Assessment of different kinetic models of carbon dioxide transformation to methanol via hydrogenation, over a Cu/ZnO/Al2O3 catalyst, *React. Kinet. Mech. Catal,* **133 (2):** 801–823 (2021).